CrystEngComm

Accepted Manuscript

ROYAL SOCIETY OF CHEMISTRY

www.rsc.org/crystengcomm

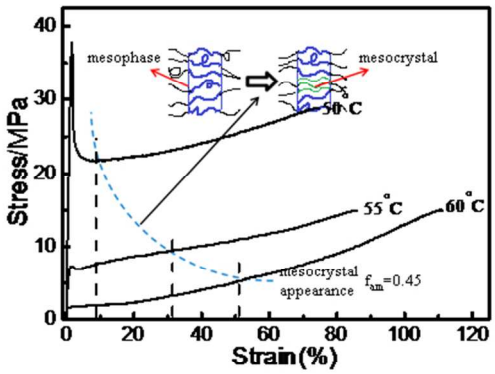

Deformation and structure evolutions of glassy poly(lactic acid) below glass transition temperature

Chengbo Zhou[a], Hongfei Li*[b], Yao Zhang[a], Feifei Xue[a], Shaoyong Huang[c], Huiying Wen[d], Jingqing Li[a], Jesper de Claville Christiansen[e], Donghong Yu[f], Zhonghua Wu[g] and Shichun Jiang*[a]

[a]*School of Materials Science and Engineering, Tianjin University, Tianjin 300072, P. R. China*

[b]*State Key Laboratory of Polymer Physics and Chemistry, Changchun Institute of Applied Chemistry, Chinese Academy of Sciences, Changchun 130022, P. R. China*

[c]*Key Laboratory of Polymer Eco-materials, Changchun Institute of Applied Chemistry, Chinese Academy of Sciences, Changchun 130022, P. R. China*

[d]*College of Engineering and Technology, Northeast Forestry University, Harbin 150040, P. R. China*

[e]*Department of Mechanical and Manufacturing Engineering, Aalborg University, DK-9220, Aalborg, Denmark*

[f]*Department of Chemistry and Biosciences, Aalborg University, DK-9220, Aalborg, Denmark*

[g]*Beijing Synchrotron Radiation Laboratory, Institute of High Energy Physics, Chinese Academy of Science, Beijing 100039, P. R. China*

* Corresponding authors: hfli@ciac.ac.cn and scjiang@tju.edu.cn

Abstract

Poly (lactic acid) (PLA) is bio-based and compostable thermoplastic polyester that has rapidly evolved into a competitive commodity material over the last decade. One key bottleneck in expanding the application field of PLA is the control of its structure and properties. Therefore, *in situ* investigations under cooling are necessary for understanding the relationship between them. The most intriguing feature of a supercooled liquid is its dramatic rise in viscosity as it is cooled toward the glass transition temperature (T_g) whereas accompanied by very little change in the structural features observable by typical X-ray experiments. The deformation behaviors and structure evolutions of glassy PLA during uniaxially stretching below T_g were *in situ* investigated by synchrotron small-angle X-ray scattering (SAXS) and wide-angle X-ray scattering (WAXS) techniques. The stretched samples were measured by differential scanning calorimetry (DSC). The obtained results showed that the deformation and yield stress of glassy PLA are strongly dependent on the stretching temperatures together with the transition of mesophase to mesocrystal and the formation of cavities. With the increase of drawing temperature, the onset of mesocrystal formation is delayed to higher strain value, whereas, corresponding to the same critical orientation degree of amorphous chains ($f_{am}\approx0.45$). The DSC results indicated that the post-Tg endothermic peak corresponding to the melting of mesocrystal appears and shifts to higher temperature with increasing stretching temperature, followed by the down-shifts (to lower temperature) of the exothermic peak of cold crystallization of PLA. The appearance of a small exothermic peak just before the melting peak related to the transition of α′ to α crystal implies the formation of α′ crystal during cold crystallization in drawn PLA samples. The structure evolution of glassy PLA stretched below T_g was discussed in details.

1. Introduction

In the temperature region below T_g, the segments of polymer chains are in "frozen" state. Only the secondary relaxations induced by local motions of smaller structural units, such as main-chain sections vibration, side groups or side chains rotation, can be observed. It is hard to detect the segments or chain motions below T_g by general experimental methods due to their long relaxation time.[1] Although stretching a glassy polymer below T_g can induce a strong anisotropy at large length scale, the structure of the stretched glassy polymer chains at the monomer scale still remains nearly isotropic with a slightly distortion. [2, 3] In other words, the structure variations and transitions of polymer chains occur slightly within temperature range below T_g. However, the viscosity of supercooled liquid and glass of polymers increases dramatically as it is cooled towards and even far below the glass transition temperature.[4, 5] Furthermore, the blown films of poly (D, L) lactide uniaxially stretched below T_g exhibit a ductile/fragile transition between 35 ^oC and 45 ^oC.[6] Therefore, it is necessary to understand the phenomenon of small structural changes corresponding to pronounced property variations of polymer glass below T_g. In addition, the T_g of PLA is in a range that makes it an idea and representative material for studying the structure evolution from glassy state of a polymer glass.

PLA is a biodegradable and biocompatible polymer with renewable carbon sources, excellent mechanical properties and well clarity,[7, 8] and can be used as bio-implants, surgical structural materials, controllable drug delivery carriers and biodegradable package, leading it to be one of the most potential alternatives for conventional petroleum-based polymers.[9, 10] For its limiting applications due to the brittleness at room temperature, PLA is usually blended with plasticizers to modify the brittle behavior for improving application performance.[11, 12] The mechanical and thermal properties of polymers are strongly dependent on the temperature related structure evolution and the resulting structure induced by various processing conditions, including temperature, shearing, stretching and pressure.[7, 10, and 13−23] Therefore, it is important to understand the structure evolution and the relationship between the structures and properties of PLA.

It is generally believed that melt crystallization of polymers is controlled by the nucleation and growth process to form the structure containing both amorphous and crystalline regions. Recently, it was reported that melt crystallization of polymers

does not occur directly from melt into crystalline phase, but *via* a pre-ordered amorphous phase named mesophase.[24–26] The crystallization of PLA from melt was considered passing through the mesophase into the crystalline forms, as proposed by Strobl et al.[27] and Wasanasuk and co-workers.[28] On the other hand, the melt-quenched PLA is not the perfectly amorphous state but it forms the mesophase containing the disordered aggregation of (10/3) helical chain segments, which can regularize into crystalline phase upon annealing.[28, 29] Mano et al.[30, 31] and Iannace et al.[32] speculated about the existence of a rigid amorphous phase apart from the mobile amorphous phase in crystalline PLA, in which the former could be the mesophase. Therefore, the mesophase is the key phase to the structure transitions of PLA from either its molten state or glassy state.

It was considered that the mesophase of PLA was related to the formation of the structure under suitable stretching conditions. Mulligan et al.[33] reported the appearance of a nematic-like order upon stretching amorphous PLA films at lower temperatures and/or higher deformation rates to high deformation levels without crystal formation, which was assigned to the highly suppression of chain relaxation process during stretching. Stoclet et al.[34–36] explored that the mesophase can be found no higher than 70 ^{o}C by stretching amorphous PLA and chain relaxation must be restricted during stretching to get high chain orientation for mesomorphic ordering. Zhang et al.[37] identified the existence of mesophase with a characteristic band at 918cm^{-1} in the PLA samples drawn at 65 ^{o}C by means of FTIR. By drawing the poly(L-lactide) and poly(D,L-lactide) (PLLA/PDLLA) blends below T_g, the less cohesive mesophase was confirmed due to the presence of amorphous PDLLA which prevents oriented segments from close intermolecular packing.[38]

Furthermore, the evolution of mesophase has significant influences on the final structure formation and properties of PLA.[34–36, 39–43] Stoclet et al.[34–36] and Na et al.[39] pronounced a sharp endotherm post-T_g in the DSC traces of PLA drawn near T_g and it could be assigned to the melting of mesophase. With the draw ratio increasing the post-T_g endothermic peak temperature shifted to higher value due to higher thermal stability, giving rise to an earlier onset of subsequent cold crystallization. Maspoch et al.[40] showed that the tensile properties (modulus, tensile strength, strain at yield and break) of the as-stretched PLA consisting of mesophase increased compared to the isotropic amorphous PLA. Wang et al.[41] reported an unusual structural evolution of drawn PLA film initially containing the oriented mesophase in annealing process. It

indicated that upon annealing the mesophase in the sample drawn to lower strain was melted more quickly and released the constraint on the oriented amorphous chains relaxation that is necessary for crystalline ordering, resulting in a more ordered crystal structure. Therefore, it is convinced that the evolution of the strain-induced mesophase of PLA can provide a way for controlling the structure and properties of PLA products.

Based on the reported results, one can know that the mesophase appears in both the crystallization and stretching process of polymers. The mesophase appeared in crystallization process is formed by unoriented amorphous chains and refers to the necessary "transition state" from the amorphous to crystalline phase,[24-29] whereas that formed in stretching process is the strain-induced intermediate phase between the amorphous and crystalline phase, composed of highly oriented amorphous chains. Moreover, the term "mesophase" could also been used to describe the confined interface layer between the crystalline and amorphous regions in semi-crystalline polymers. [29-32] Therefore, for distinguishing these different intermediate structures, we prefer to consider the strain-induced intermediate phase as a more ordered mesocrystal rather than mesophase in present study. Furthermore, the mesocrystal was evolved from the mesophase initially existed in the glassy PLA considering that the melt-quenched PLA is not necessary the perfectly amorphous state but contains the mesophase [28].

Although many studies have revealed the structure evolutions and property variations of PLA under various stretching conditions, the structure evolution of glassy PLA stretched below T_g has not yet been understood completely. In the present study, the deformation behaviors and the structure formations of glassy PLA drawn at 50−60 ^{o}C were investigated by means of *in situ* synchrotron SAXS and WAXS techniques combined with DSC measurements. By analyzing the structural feature changes of glassy PLA during stretching, we considered that the strain-induced intermediate phase as a more ordered mesocrystal rather than a mesophase. Furthermore, the mesocrystal was formed from the mesophase, which is corresponding to the rigid amorphous phase coexisting with mobile amorphous phase in the glassy PLA.

2. Experimental section

2.1. Material and sample preparation

Poly (lactic acid) (PLA) containing 0.8 wt% of D-isomer units was obtained from Zhejiang Hisun Biomaterials Co., Ltd (China). The number average molecular weight (M_n) and polydispersity index (*PDI*) is 88.2 × 10^3 g/mol and 1.24, respectively. The glass transition temperature (T_g), crystallization temperature (T_c), and melting point (T_m) determined by DSC is 63.5 °C, 102.3 °C and 176.4 °C, respectively.

PLA granules were dried in vacuum oven at 50 °C for 24 hours. Then the dried PLA granules were melted at 200 °C and compressed into sheet with thickness of about 0.5 mm, followed by the immediate quenching into ice water to obtain glassy PLA sheet. Dumbbell-shaped sample bars with dimensions of 26.0 mm (gauge length) × 3.0 mm (neck length) × 2.1 mm (neck width) were cut from PLA sheet for the *in situ* structure and property determinations. Before the tensile deformation measurements, the dumbbell-shaped samples cut from the quenched sheet were dried in vacuum oven at 30 °C for enough time again to remove the residual water.

2.2. Tensile measurements

The glassy PLA bars were stretched uniaxially by using a Linkam TST350 hot tensile stage (Linkam Scientific Instruments, Ltd., U.K.), which allows symmetrical stretching so that the same part of the sample always remains in the way of the incident beam. The deformation measurements were carried out at 50 °C, 55 °C, and 60 °C, which were below T_g of PLA, at a stretching rate of 4μm/s for obtaining engineering stress-strain curves.

2.3. Synchrotron SAXS and WAXS measurements

In situ synchrotron small angle X-ray scattering (SAXS) and wide angle X-ray scattering (WAXS) measurements of the amorphous PLA samples stretched with the same stretching rate and tensile device as part 2.2 at different temperatures were performed at beamline 1W2A (λ=0.154 nm) of Beijing Synchrotron Radiation Facility (BSRF),[44] Beijing, China. Mar165-CCD detector was adopted to collect scattering data with sample-detector distance of 1595 mm and 98 mm for SAXS and WAXS measurements, respectively. Since the X-ray intensity of BSRF (Beijing Synchrotron Radiation Facility) is damped with time in a period of 6h and the thickness of stretched samples is decreasing with strain increasing, the expose time of SAXS/WAXS measurements was adjusted from time to time to obtain the data with

proper intensity. The expose time ranges for SAXS and WAXS measurements were 10s-80s and 20-60s, respectively. The corresponding background of the air and tensile device between sample and detector was also recorded. All of the 2D-patterns were normalized firstly to reduce the effects of the changes in the X-ray source intensity and sample thickness, and then were subtracted the background scattering, lastly integrated into 1D intensity profiles along the equatorial and meridional directions with fit2d software.[45]

2.4. Differential scanning calorimetry

The deformed PLA samples after stretching were measured by DSC (DSC-Q20, from TA Company) with a rate of 10 ^{o}C /min. The glass transition temperatures and crystallization temperatures of drawn PLA samples were obtained from the first heating process.

3. Results and discussion

3.1. Deformation behaviors of PLA at different temperatures

The deformation behaviors of glassy PLA were observed at 50 ^{o}C, 55 ^{o}C, and 60 ^{o}C, below T_g, with TST350 hot tensile stage. The obtained engineering stress-strain curves reveal that deformation properties of glassy PLA are strongly influenced by stretching temperatures, as shown in Fig. 1. Drawn at 50 ^{o}C, the stress-strain curve (SSC) represents a typical deformation behavior of polymer, including the elastic deformation region with high slope, yielding region with negative slope, and strain hardening region with moderate positive slope.[46] It shows an elastic deformation with a high Young's modulus within the low strain range of about 1.8%. A pronounced strain softening with a dramatical decrease of nominal stress occurs after the yield point. The strain hardening behavior can be observed with stress increasing again after strain softening. The deformation behavior of PLA stretched at 55 ^{o}C is comparable to that at 50 ^{o}C with the smaller stress at same strain and the strain softening behavior becoming much weaker. Drawn at 60 ^{o}C, just below T_g, the SSC is completely different from those at 50 ^{o}C and 55 ^{o}C. It shows a rubber-liked deformation behavior with an initial low platform followed by a strain hardening. The stress becomes much lower and the strain softening phenomenon is too weak to be observed. The deformation behaviors of glassy PLA are distinct at different stretching temperatures below T_g, especially the yield stress and the strain softening process.

The glassy PLA below T_g can be considered as supercooled liquid whose viscosity increases dramatically with temperature decreasing,[4, 5] due to the enhanced vitrification effect on segments. With the increase of drawing temperature the vitrification of segments becomes weaker, lower stress can overcome the energy barrier and induce the yielding[47] of the frozen segments, so the yield stress of glassy PLA drops drastically. It is noteworthy that, due to the broad *PDI* of 1.24 of PLA studied, some of PLA chains have the lower molecular weight than M_n of 88.2Kg/mol, correspondingly have the lower T_g than 60 ^oC, very close to the T_g measured by DSC. In the case of 60 ^oC, these PLA chains with lower T_g are in the rubbery state and can be viewed as the "plasticizer" for PLA sample, which will decrease the vitrification of segments significantly, therefore leading to a much lower yield stress for PLA sample drawn at 60 ^oC. On the other hand, the different amplitude of strain softening is related to the formation and growth of cavities at different stretching temperatures,[48] which will be discussed in more details in next section.

The structures of polymers in the temperature range below T_g are almost the same and difficult to transform into other forms owing to the "frozen" chains and segments with very long relaxation time.[1, 4, 5] As shown in Fig. 2, the SAXS and WAXS results of undrawn PLA samples at stretching temperatures below T_g are almost the same except for the scattering intensity due to the difference of sample thickness, which implies that all of the undrawn PLA samples are amorphous and the structure of them has little changes at different drawing temperatures below T_g. However, the temperature related deformation behaviors of glassy PLA below T_g are different, as shown in Fig 1. *In situ* SAXS and WAXS measurements are necessary to understand the phenomenon of little structural changes corresponding to obvious variations of property of glassy PLA stretched below T_g.

3.2. *In situ* SAXS and WAXS analysis of PLA stretched at different temperatures

To understand the structure evolution with dramatic property changes of PLA at the stretching temperatures below T_g, *in situ* SAXS and WAXS measurements of PLA drawn at 50 ^oC, 55 ^oC, and 60 ^oC were performed with synchrotron X-radiation. Engineering stress–strain curves and selected 2D SAXS and WAXS patterns collected during uniaxial tensile deformation of PLA at 50 ^oC and 60 ^oC are illustrated in Fig. 3. Both of SAXS and WAXS patterns of undrawn PLA samples are isotropic, proving that there are no oriented structures in the undrawn samples. When the sample was subjected to stretching at 50 ^oC, a strong streak of SAXS pattern inclined to draw axis

with an angle of about 30° firstly appeared before the yield point, as shown in Fig. 3a and 3c. Subsequently, an intense streak was also observed in the direction perpendicular to the previous one. These streaks are related to the voided structures and arise from the scattering between the polymer matrix and voids.[49] Moreover both of the streaks are normal to each other, being similar to the characteristic of shear banding of amorphous polymers during cold drawing. However, the shear banding is not involved the changes in sample volume. [49] Therefore it is convinced that these streaks originated from the scattering of sheared voids inclined to draw direction. During the strain softening stage, the angle between the both streaks decreases, i.e. smaller than 90°. The streak in the meridional direction becomes stronger and get oriented long meridian, indicating that the voids get oriented along the draw direction gradually. With strain further increasing, the SAXS pattern of criss-cross streak develops gradually into a vertical streak, roughly orthogonal to the draw direction, which means that all of the inclined cavities transform into the ones parallel to the draw direction.[9, 50] Entering into the strain hardening stage, the vertical streak changes little because of cavities parallel to draw direction becoming stable gradually.

The SAXS patterns of PLA stretched at 60 °C, just below T_g, have little changes within the strain range below 20%, as shown in Fig. 3b. It is of note that, unlike drawn at 50 °C, no elongated streaks normal to each other appears in SAXS patterns. Correspondingly there are no voids emerged and the deformation is homogenous, which could be attributed to the high enough plasticity of PLA due to the lower molecular weight PLA "plasticizer" appeared at 60 °C.[51] With further stretching, a very weak streak along the meridional direction appears gradually at large strain range, caused by the formation of a small amount of cavities along draw direction due to large enough extension of amorphous phase. The SAXS patterns of PLA stretched at 55 °C are almost the same as that at 50 °C, which is consistent with the similar deformation behaviors in their SSCs. However, the intensity of the streaks related to the cavitation is much weaker than that at 50 °C. Therefore, the formation and growth of cavities of PLA stretched at 55 °C is less significant than that at 50 °C due to the higher plasticity of PLA.

The SAXS results indicate that glassy PLA samples are subjected to different cavitations at drawing temperatures below T_g, which results in the different strain softening process.[48] Stretched at 50 °C, a significant cavitation of PLA occurs due to high plastic resistance at low stretching temperature, which could induce a sharp yield

behavior.[52] Upon drawing, large number of elongated voids inclined to draw direction form firstly. Reaching to yield point, the elongated voids become the defect points of internal stress and get themselves oriented along draw direction. The orientation of the inclined cavities results in a quick reduction of sample cross-section as a result of plastic instability, i.e. necking, which induces large decrease of nominal stress, i.e., a sharp strain softening. With drawing temperature increasing the plastic resistance of PLA decreases, so the cavitation becomes less pronounced leading to the much weaker strain softening behavior, especially strain softening disappeared at 60 ^{o}C due to the lower molecular weight PLA "plasticizer".

WAXS patterns of PLA drawn at 50 ^{o}C have little changes and remain almost isotropic scattering halo before yield, as shown in Fig. 3a and 3c, which implies that the amorphous phase of PLA is unoriented at this stage. After the yield point, the scattering halo of amorphous phase disappears gradually and develops into two arcs along the meridian. The two arcs turn into two-blob like pattern with further stretching. It demonstrates that amorphous phase of PLA gets high orientation gradually along stretching direction with stretching. Compared to that at 50 ^{o}C, the WAXS patterns of PLA drawn at 55 ^{o}C and 60 ^{o}C show the similar evolutions from isotropic scattering halo of amorphous phase into two arcs and then into two-blob like feature along the meridional direction with strain increasing. The similar changes of WAXS patterns during stretching were also reported by studies of Stoclet et al.,[34, 35] which was assigned to the orientation of amorphous chains and the subsequent formation of mesophase at large enough strains. Worth noting is that the term "mesophase" have also been used to describe the necessary "transition state" from the amorphous to crystalline phase in crystallization process of polymers[24-29] and the confined interface layer (rigid amorphous phase) between the crystalline and amorphous regions in semi-crystalline polymers[29-32]. Therefore, to distinguish these different intermediate structures, we prefer to consider the strain-induced intermediate phase as a more ordered mesocrystal rather than mesophase in present study. Furthermore, the mesocrystal was formed from the mesophase initially existed in the glassy PLA given that the melt-quenched PLA is not necessary the perfectly amorphous state but contains the mesophase [28].

The 1D WAXS profiles along the equatorial direction and the meridional direction at the related strain of PLA drawn at the indicated temperatures are shown in Fig. 4. Drawn at 50 ^{o}C, the scattering peak of amorphous phase of PLA along the equatorial

direction decreases gradually and disappears eventually with strain increased, while the scattering peak along the meridional direction becomes much sharper and stronger, which indicates that more and more amorphous segments get oriented along tensile direction resulting in formation of mesocrystals. 1D WAXS intensity profiles along the equatorial and meridional direction of PLA drawn at 55 ^{o}C and 60 ^{o}C have similar variations to that of PLA stretched at 50 ^{o}C. However, the equivalent degree of orientation of amorphous phase is delayed and shifts to the larger strain value due to a higher dynamics of segments relaxation[34] of PLA stretched at 55 ^{o}C and 60 ^{o}C, as shown in Fig. 4b and 4c.

To analyze in detail the variations of the contents of mesocrystal and amorphous phase and the orientation degree of amorphous chains of PLA stretched at different temperatures and the relationship between them, the contents of mesocrystal and amorphous phase, X_{meso} and X_{am}, were obtained by fitting 1D WAXS profiles along the meridional direction using the Jade 6.0 peak fitting software, in the process of which assuming Gaussian profiles for all scattering peaks and amorphous halo. The fitting method was outlined by Stoclet et al.[34, 35] Two examples of fitting meridian integrated WAXS profiles of PLA samples before stretching and drawn at 50 ℃ up to ε ≈112.2% are shown Fig. 5. The content of one phase (amorphous phase, or mesocrystal) was calculated by the area ratio of diffraction peaks from the phase and total scattering peaks. Amorphous chain orientation was obtained from 360^{o} azimuth integration of the 2D WAXS patterns by using the main amorphous halo with scattering peak at about 2θ =15.5^{o} [34]. The degree of orientation of the amorphous phase was calculated according to the Herman's orientation function.[33]

$$f = \frac{3(\cos^2\phi) - 1}{2} \tag{1}$$

where, Φ is the angle between the chain axis and the reference axis (stretching direction), and $\cos^2\Phi$ is defined as:

$$\cos^2\phi = \frac{\int_0^{\frac{\pi}{2}} I(\phi)\cos^2(\phi)\sin(\phi)d\phi}{\int_0^{\frac{\pi}{2}} I(\phi)\sin(\phi)d\phi} \tag{2}$$

where, $I(\Phi)$ is the scattering intensity along the angle Φ.

The changes of mesocrystal content, X_{meso}, amorphous phase content, X_{am} and orientation degree of amorphous chains, f_{am}, with strain in stretched glassy PLA at the

fitted temperatures are shown in Fig. 6. Drawn at 50 °C, the f_{am} increases abruptly at the yield point indicating a plastic instability or necking involving a heterogeneous deformation along the sample,[34] and continues to increase at strain softening stage, as shown in Fig. 6a. The mesocrystal appears at the strain near 8.3% with f_{am} of about 0.45 corresponding to the completion of strain softening. Then the mesocrystal increases gradually up to 16% with f_{am} increasing continuously. The degree of chain orientation of amorphous PLA stretched at 55 °C turns out to be lower value at the same strain compared with that at 50 °C because of a higher dynamics of segments relaxation, which leads to a larger initial strain (about 32.6%) of mesocrystal appearance, as shown in Fig. 6b. Upon drawing at 60 °C, with f_{am} increasing the mesocrystal do not appear until the f_{am} increases up to about 0.45 at strain about 52.6%, and then mesocrystal content increases rapidly and levels off at the strain larger than 100%, as shown in Fig. 6c.

By comparing the results in Fig. 6a, 6b and 6c, it is found that the initial strain for mesocrystal appearance is delayed to higher value with drawing temperature increasing, corresponding to 8.3%, 32.6%, and 52.6% at 50 °C, 55 °C, and 60 °C, respectively. The phenomenon is due to a higher segments relaxation at higher drawing temperature that delays the initial chains getting oriented and ordering into mesocrystal.[34] It is confirmed by the orientation degree of amorphous phase of PLA drawn at different temperatures. The orientation degree of amorphous phase at higher temperatures is lower than that at lower temperatures with the same strain, as shown in Fig 6. Therefore a higher initial strain is required for amorphous segments to get enough orientation to form mesocrystal at higher drawing temperature. Furthermore, we speculate that a quantitative relationship exists between the initial strain and the drawing temperature in the temperature range studied. Fig. 7 is the variation of initial strain, ε_{int}, with the logarithm of drawing temperature, $\log T_d$, and the fitting data of them. It proves that there is a linear relationship between ε_{int} and $\log T_d$ within the studied temperature range. This linearity would be helpful to understand the temperature dependent structure transition of glassy PLA during stretching. On the other hand, despite with different ε_{int} at different T_d, a critical orientation degree of amorphous phase of all the measured samples corresponding to mesocrystal appearance is observed at 0.45. Therefore we speculate that the mesocrystal is not a simple oriented amorphous phase but a cohesive phase with specific chain conformation and thermal properties, which has been confirmed by previous studies.[34,

[37, 39] A characteristic band at about 918 cm^{-1} of FTIR spectroscopy corresponding to the chain conformation was found for mesocrystal appearance.[34, 37, 39] Stoclet et al. determined a specific melting enthalpy ΔHm^{meso} of about 70 J/g and a "melting" point of about 75 ^{o}C for PLA mesocrystal.[34]

To explore in more details the process of mesocrystal formation from amorphous phase in the stretched glassy PLA at meso-scale, the correlation length of PLA mesophase during stretching was calculated with the 1D SAXS profiles ($I(q)$-q plots) within the small q range according to the Debye−Bueche Plot:[53]

$$1/I(q) = [\,1/A + (\xi/A)\,q^2\,]^2 \qquad (3)$$

where, A is a constant and ξ is a correlation length. From the plots $I(q)^{-1/2}$ versus q^2, the ξ can be obtained as a ratio of the slope and intercept of straight line.

The variations of correlation length of mesophase, ξ, of PLA stretched at the fixed temperatures together with X_{meso} and X_{am} are shown in Fig. 8. The initial value of correlation length of mesophase in glassy PLA is about 14nm. Although the correlation length of PLA mesophase exhibits the different variation trends at different drawing temperatures, the turning points of the mesophase correlation length perpendicular to stretching direction, ξ_e, are all corresponding to the onset of mesocrystal appearance. We consider that the amorphous phase and mesophase coexist in the sample of melt-quenched PLA glass, and the mesocrystal is formed in the mesophase during stretching. Upon stretching at 50 °C, the elongated voids inclined to stretching direction are formed in the amorphous phase and develops rapidly, which leads to the fracture of the mesophase and the separation of the broken mesophase along draw direction. Therefore the amount of mesophase perpendicular to draw direction becomes smaller and the correlation length in this direction, ξ_e, increases dramatically, while that along the draw direction, ξ_m, decreases drastically due to the increased mesophae in the stretching direction. With further deformation the elongated cavities inclined to stretching direction get oriencted along draw axis rapidly, resulting in a quick reduction of sample cross-section, which leads to the rapid decrease of ξ_e. However, the correlation length along draw direction, ξ_m, gradually increases due to the increased strain. After the strain softening, most of the inclined cavities transform into the elongated ones along draw direction and become stable gradually. The decrease of ξ_e becomes slow abruptly, leading to the appearance of turning ponit of ξ_e. The ξ_m continues to increase with the strain further increasing.

Meanwhile, the segments in the mesophase are stretched to critical extent to form the mesocrystal. Thereafter the content of mesocrystal increases gradually, meanwhile the ξ_e and ξ_m change slowly with strain increasing. The variation of ξ of the mesophase and the corresponding appearance of mesocrystal of PLA drawn at 55 ^oC are similar to that at 50 ^oC, as shown in Fig. 8b, but the amplitude of the variation of ξ is smaller than that at 50 ^oC due to the less pronounced cavitation of PLA drawn at 55 ^oC.

The variation of ξ of PLA stretched at 60 ^oC is different from that at 50 ^oC and 55 ^oC, as shown in Fig. 8c. Upon drawing at 60 ^oC, the homogeneous deformation occurs and there are no cavities emerged at the early tensile stage due to a high plasticity, therefore the ξ of PLA mesophase does not has large changes. When the strain larger than 50%, the amorphous phase gets orientation high enough, a small amount of elongated cavities appears in the amorphous phase and the mesophase is broke up and then separated, leading to the abrupt increase of ξ_e and a slight decrease of ξ_m. Meanwhile the mesocrystal begins to appear in mesophase due to the high enough degree of orientation of the segments in mesophase.

To understand the structure evolution process of glassy PLA below T_g, the glassy PLA can be perceived as a hybrid structure, which is composed of a primary structure owing to the short-ranged van der Waals bonds and a chain network due to chain interpenetration and uncrossability, proposed by Wang et al.[47, 54-57] for polymer glasses of high molecular weight under large deformation below Tg. Far below T_g the glassy PLA is in a deep glassy state, segmental mobility is much low due to the strong intersegmental van der Waals forces.[54] Upon stretching, the primary structure, composed of the short-ranged intersegmental van der Waals bonds, requires a high stress to yield and transfers the large load to the load-bearing strands (LBSs) of chain network.[47] The high intra-segmental force, i.e., chain tension, builds up in LBSs. When it is high enough, some shorter strands between the two junctions in the amorphous phase can be pulled out of the chain network, inducing strain localization and the elongated cavities inclined to draw direction. The elongated cavities become the defect points and are rapidly stretched to get oriented along draw direction, leading to the sharp strain softening. After most of the cavities turn into the elongated ones along the stretching direction and gradually become stable, the longer LBSs that have not yet been pulled out from chain network continue to be extended and the chain tension in LBSs increases again, initiating the strain hardening. The chain segments in the mesophase are continually stretched to a critical level to form a meso-

ordered structure, i.e., mesocrystal. With the drawing temperature increasing, the primary structure becomes weaker and a lower stress can make it breakdown. The lower load is transferred to LBSs of chain network, leading to the buildup of the lower chain tension.[56] Consequently, less LBSs can be pulled out from the chain network, producing a smaller amount of cavities and correspondingly the less significant strain softening, even disappearance of strain softening at 60 ^{o}C due to the much weaker primary structure. Since the segmental mobility is higher at higher drawing temperatures, the segments relaxation occurs more readily during stretching. Therefore, the segments in the mesophase get oriented more slowly in the post-yielding regime, which requires the larger strain to get enough orientation for the formation of mesocrystal.

It is known that little structure variations of glassy PLA can occur at temperatures below T_g with the "frozen" segments. As mentioned above, the glassy PLA stretched below T_g could form mesocrystal even though with the low kinetics of chain ordering. It may be attributed to a weak increase of local temperature generated in deformation zone,[34] originating from the heat released by the internal energy stored in LBSs during deformation.[57] However, the weak increase of local temperature was not high enough to make the stretched chains order into more ordered crystals.

Based on the above discussion, a schematic mechanism was established to illustrate the structure evolution of glassy PLA uniaxially stretched at 50 ^{o}C and 60 ^{o}C, as shown in Fig. 9. Drawn at 50 ^{o}C, lots of elongated cavities inclined to stretching direction emerges before yield point due to high plastic resistance, breaking up and separating the mesophase and leading to the dramatic increase of ξ_e and the decrease of ξ_m. After yield point, the elongated cavities inclined to stretching direction transforms into the horizontal ones rapidly, leading to the heterogeneous deformation and rapid reduction of sample cross-section. The ξ_e begins to decrease drastically, whlie the ξ_m begins to increase gradually. After strain softening, most of the cavities change into the elongated ones along the draw direction and become stable, the decrease of the ξ_e becomes slowdown and the segments in mesophase are stretched to critical extent to form mesocrystal. The content of mesocrystal increases gradually with orientation degree of amorphous phase increasing at the strain hardening stage. Upon drawing at 60 ^{o}C, the homogeneous deformation of PLA occurs and there are no cavities emerged at the early tensile stage due to a high plasticity. Therefore the ξ of PLA mesophase has a little change and only an obvious orientation of amorphous

chains occurs. At intermediate strain range, a small amount of voids appears, leading to the breaking and separating of the mesophase and the abrupt increase of ξ_e. Meanwhile, mesocrystal begins to form with the segments in mesophase stretched enough and increases gradually at latter stage of strain hardening.

3.3. Thermal property of deformed PLA samples

The thermal property of the strain-induced structure of PLA has been measured by DSC as a function of drawing temperature. Fig. 10 shows the DSC heating curves of the deformed PLA after drawing at 50 ^{o}C, 55 ^{o}C, and 60 ^{o}C, and for the sake of comparison the DSC trace of undrawn PLA sample is also included here. For undrawn PLA sample, a typical step change of glass transition is observed. Subsequently, a broad exothermic peak of cold crystallization within temperature range of about 85 ^{o}C to 140 ^{o}C appears. In particularly, a small exothermic peak just prior to the melting peak is observed, which is attributed to the transition of disordered α′ crystal formed during cold crystallization to the ordered α crystal.[7, 8, 34]

For PLA samples drawn at different temperatures, a pronounced post-T_g endothermic peak is observed, which could be assigned to the melting of the cohesive mesocrystal with a certain chain ordering rather than the enthalpy recovery of physical aging or relaxation of chain orientation.[34, 39, 41] Moreover, with drawing temperature increasing, the post-T_g endothermic peak becomes much sharper and shifts to higher temperatures, indicating that the mesocrystal with higher thermal stability and cohesive strength could be formed at higher drawing temperature.[34, 39] In contrast, the subsequent cold crystallization exotherm initiates at lower temperature with drawing temperature increasing. It is surprising that the small exotherm prior to melting peak decreases and disappears gradually, i.e., the transition of α′ to α form becomes unobvious in the sample stretched at higher temperature.

From above, one can know that the thermal properties of PLA samples drawn at different temperatures shows obvious changes. It may be attributed to the distinct structure evolution of PLA stretched at different temperatures as described in the preceding section. At lower drawing temperature, the segments mobility is lower, therefore the resulting mesocrystal may be a looser packing of interchain,[37] which leads to a lower thermal stability. In contrast, at higher drawing temperature, the more ordered mesocrystal[41] with a closer interchain packing are formed and could be preserved to a large extent during glass transition, which could give rise to an earlier onset of cold crystallization.[39] Correspondingly, in the subsequent cold crystallization

process less amount of α′ crystal forms and the transition of α′ to α crystal becomes weaker, leading to the gradually disappearance of the small exotherm just prior to melting peak.

4. Conclusions

Deformation behaviors and structure evolutions of amorphous PLA stretched at 50−60 ^{o}C were investigated by a tensile hot stage, *in situ* synchrotron SAXS and WAXS measurements. With drawing temperature increasing, the yield stress becomes much lower due to the weaker vitrification of segments. And the stain softening becomes much less significant and even disappears at 60 ^{o}C, which could be attributed to that less elongated cavities inclined to draw direction are formed and develops into the elongated horizontal ones due to the higher plasticity at higher drawing temperatures. At strain hardening stage, mesocrystal begins to appear in the mesophase with the orientation degree of amorphous phase further increasing and the appearance of turning points of the mesophase correlation length perpendicular to draw direction. The initial strain of mesocrystal appearance, ε_{int}, shifts to a higher value with increasing drawing temperature, caused by the detrimental effect of chain relaxation on chain orientation necessary to form mesocrystal at higher drawing temperature. A linear relationship exists between ε_{int} and logT_d within the studied temperature range. It is of note that the mesocrystal begins to appear with a critical orientation degree of amorphous phase of about 0.45, despite with different initial strain of mesocrystal appearance. It means that only when molecular chains in the amorphous phase get high enough orientation degree can the stretched segments in mesophase be transformed into mesocrystal, which is not a simple oriented amorphous phase, but a cohesive phase with certain molecular ordering and conformation.

Correspondingly, the thermal properties of glassy PLA drawn at 50-60 ^{o}C are also different due to the different resulting structures. With drawing temperature increasing, the post-T_g endotherm of the melting of mesocrystal becomes much sharper and appears at higher temperatures because of closer interchain packing and higher cohesive strength, which subsequently triggers an earlier cold crystallization to form larger amount of ordered α crystal leading to the gradual disappearance of the small exotherm of the transition of α′ to α crystal just prior to melting peak.

Acknowledgements

This work was supported by the National Natural Science Foundation of China (21374077, 51173130 and 21274149) and the Special Funds for National Basic Research Program of China (2010CB631102).

References

1 M. T. Cicerone and M. D. Ediger, *J. Chem. Phys.*, 1992, **97**, 2156–2159.
2 F. Casas, C. Alba-Simionesco, H. Montes and F. Lequeux, *Macromolecules*, 2008, **41**, 860–865.
3 F. Casas, C. Alba-Simionesco, F. Lequeux and H. Montes, *J. Non-Cryst. Solids*, 2006, **352**, 5076–5080.
4 M. L. Williams, R. F. Landel and J. D. Ferry, *J. Am. Chem. Soc.*, 1955, **77**, 3701– 3707.
5 J. C. Mauro, Y. Z. Yue, A. J. Ellison, P. K. Gupta and D. C. Allan, *Proc. Natl. Acad. Sci. U.S.A.*, **2009**, **106**, 19780–19784.
6 G. Stoclet, S. Elkoun, V. Miri, R. Seguelal and J. M. Lefebvre, *Int. Polym. Process.*, 2007, **22**, 385–388.
7 S.Y. Huang, H. F. Li, S. C. Jiang, X. S. Chen, and L. J. An, *Polymer*, 2011, **52**, 3478–3487.
8 S. Saeidloua, M. A. Huneaulta, H.B. Li and C. B. Park, *Prog. Polym. Sci.*, 2012, **37**, 1657–1677.
9 X. Q. Zhang, K. Schneider, G. M. Liu, J. H. Chen, K. Brüning, D. J. Wang and M. Stamm, *Polymer*, 2011, **52**, 4141–4149.
10 P. T. Xiao, H. F. Li, S. Y. Huang, H. Y. Wen, D. H. Yu, Y. R. Shang, J. Q. Li, Z. H. Wu, L. J. An and S. C. Jiang, *Cryst. Eng. Comm.*, 2013, **15**, 7914–7925.
11 R. L. Yu, L. S. Zhang, Y. H. Feng, R. Y. Zhang and J. Zhu, *Chin. J. Polym. Sci.*, 2014, **32**, 1099–1110.
12 Y. P. Hao, H. H. Ge, L. J. Han, H. L. Zhang and L. S. Dong, *Chin. J. Polym. Sci.*, 2013, **31**, 1519–1527.
13 B. Kalb and A. J. Pennings, *Polymer*, 1980, **21**, 607–612.
14 J. M. Zhang, Y. X. Duan, H. Sato, H. Tsuji, I. Noda, S. K. Yan and Y. Ozaki, *Macromolecules*, 2005, **38**, 8012–8021.
15 W. Hoogsteen, A. R. Postema, A. J. Pennings and G. Brinke, *Macromolecules*, 1990, **23**, 634–642.
16 B. Eling, S. Gogolewski and A. J. Pennings, *Polymer*, 1982, **23**, 1587–1593.
17 D. Sawai, K. Takahashi, A. Sasashige and T. Kanamoto, *Macromolecules*, 2003, **36**, 3601–3605.

18 L. Cartier, T. Okihara, Y. Ikada, H. Tsuji, J. Puiggali and B. Lotz, *Polymer*, 2000, **41**, 8909–8919.
19 Z. W. Cai, Y. Zhang, J. Q. Li, F. F. Xue, Y. R. Shang, X. H. He, J. C. Feng, Z. H. Wu and S. C. Jiang, *Polymer*, 2012, **53**, 1593–1601.
20 X. Q. Zhang, K. Schneide, G. M. Liu, J. H. Chen, K. Brüning, D. J. Wang and M. Stamm, *Polyme*r, 2012, **53**, 648–656.
21 H. L. Guo, Y. Zhang, F. F. Xue, Z. W. Cai, Y. R. Shang, J. Q. Li, Y. Chen, Z. H. Wu and S. C. Jiang, *Cryst. Eng. Comm.*, 2013, **15**, 1597–1606.
22 C. D. Qiao, S. C. Jiang, X. L. Ji and L. J. An, *Chin. J. Polym. Sci.*, 2013, **31**, 1321–1328.
23 S. Y. Huang, H. F. Li, D. H. Yu, S. C. Jiang, X. S. Chen and L. J. An, *Cryst. Eng. Comm.*, 2013, **15**, 4372–4378.
24 S. Sasaki, K. Tashiro, M. Kobayashi, Y. Izumi and K. Kobayashi, *Polymer* **1999**, *40*, 7125–7135.
25 G. Strobl, *Eur. Phys. J. E*, 2000, **3**, 165–183.
26 G. Strobl, *Prog. Polym. Sci.*, 2006, **31**, 398–442.
27 T. Y. Cho and G. Strobl, *Polymer*, 2006, **47**, 1036–1043.
28 K. Wasanasuk and K. Tashiro, *Macromolecules*, 2011, **44**, 9650–9660.
29 J. M. Zhang, Y. X. Duan, J. Abraham and Y. Ozaki, *Macromolecules*, 2010, **43**, 4240–4246.
30 J. F. Mano, *J. Non-Cryst. Solids*, 2007, **353**, 2567–2572.
31 J. F. Mano, Y. M. Wang, J. C. Viana, Z. Denchev and M. Oliveira, *Macromol. Mater. Eng.*, 2004, **289**, 910–915.
32 S. Iannace and L. Nicolais, *J. Appl. Polym. Sci.*, 1997, **64**, 911–919.
33 J. Mulligan and M. Cakmak, *Macromolecules*, 2005, **38**, 2333–2344.
34 G. Stoclet, R. Seguela, J. M. Lefebvre and C. Rochas, *Macromolecules*, 2010, **43**, 7228–7237.
35 G. Stoclet, R. Seguela, J. M. Lefebvre, S. Elkoun and C. Vanmansart, *Macromolecules*, 2010, **43**, 1488–1498.
36 G. Stoclet, R. Seguela, C. Vanmansart, C. Rochas and J. M. Lefebvre, *Polymer*, 2012, **53**, 519–528.
37 J. Hu, T. P. Zhang, M. G. Gu, X. Chen and J. M. Zhang, *Polymer*, 2012, **53**, 4922–4926.
38 R. H. Lv, S. F. Zou, B. Na, H. Y. Pan and H. Y. Deng, *Polym. Eng. Sci.*, 2013, **53**, 21–26.
39 R. H. Lv, B. Na, N. N. Tian, S. F. Zou, Z. J. Li and S. C. Jiang, *Polymer*, 2011, **52**, 4979–4984.
40 J. C. Velazquez-Infante, J. Gamez-Perez, E. A. Franco-Urquiza, O. O. Santana, F.

Carrasco and M. L. Maspoch, *J. Appl. Polym. Sci.*, 2013, **127**, 2661–2669.
41 Y. M. Wang, M. Li, K. J. Wang, C. G. Shao, Q. Y. Li and C. Shen, S*oft Matter*, 2014, **10**, 1512–1518.
42 R. H. Lv, S. F. Zou, B. Na, H. Y. Deng and Z. W. Yu, *Polym. Eng. Sci.*, 2013, **53**, 2568–2572.
43 Q. Ma, M. Pyda, B. Mao and P. Cebe, *Polymer*, 2013, **54**, 2544–2554.
44 Z. H. Li, Z. H. Wu, G. Mo, X. Q. Xing and P. Liu, *Inst. Sci. Technol.*, 2014, **42**, 128–141.
45 Z. H. Li, *Chin. Phys. C*, 2013, **37**, 110–125.
46 T. Kamal, T. J. Shin and S. Y. Park, *Macromolecules*, 2012, **45**, 8752–8759.
47 S. W. Cheng, L. Johnson and S. Q. Wang, *Polymer*, 2013, **54**, 3363–3369.
48 S. Castagnet, S. Girault, J. L. Gacougnolle and P. Dang, *Polymer*, 2000, **41**, 7523–7530.
49 G. Stoclet, J. M. Lefebvre, R. Séguéla and C. Vanmansart, *Polymer*, 2014, **55**, 1817–1828.
50 J. Wu and J. M. Schultz, *Macromolecules*, 2000, **33**, 1765–1777.
51 A. Pawlak and A. Galeski, *Macromolecules*, 2005, **38**, 9688–9697.
52 S. Castagnet, J. L. Gacougnolle and P. Dang, *Mater. Sci. Eng. A*, 2000, **276**, 152–159.
53 K. R. Reddy, K. Tashiro, T. Sakurai, N. Yamaguchi, S. Sasaki, H. Masunaga and M. Takata, *Macromolecule*s, 2009, **42**, 4191–4199.
54 G. D. Zartman, S. W. Cheng, X. Li, F. Lin, M. L. Becker and S. Q. Wang, *Macromolecules*, 2012, **45**, 6719–6732.
55 S. W. Cheng and S. Q. Wang, *Phys. Rev. Let.*, 2013, **110**(065506), 1–4.
56 S. W. Cheng and S. Q. Wang, *Macromolecules*, 2014, **47**, 3661–3671.
57 P. P. Lin, S. W. Cheng and S. Q. Wang, *ACS Macro Lett.*, 2014, **3**, 784–787.

Figure Caption

Fig. 1 The engineering stress-strain curves of PLA stretched at 50 °C, 55 °C, and 60 °C.

Fig. 2 (a) The 2D SAXS and WAXS patterns of undrawn PLA samples at different stretching temperatures and (b) the corresponding 1D SAXS and WAXS profiles.

Fig. 3 Engineering stress–strain curves and selected 2D SAXS (1s-6s) and WAXS (1w-6w) patterns collected during uniaxial tensile deformation of PLA at (a) 50 °C, (b) 60 °C. (c) Engineering stress–strain curve within the initial 10% strain range of PLA drawn at 50 °C and the corresponding 2D SAXS and WAXS patterns. The faint scattering arcs in the equatorial direction of WAXS patterns of strains larger than 10% in Fig. 3(a) and 3(b) originated from the scattering of Linkam tensile stage. The red marks were added in part (c) to show where each SAXS/WAXS measurement started and finished. The stretching direction is horizontal and is defined as equator hereafter.

Fig. 4 1D WAXS intensity profiles along the equatorial direction and the meridional direction at the related strain of PLA stretched at (a) 50 °C, (b) 55 °C and (c) 60 °C. For clarification vertical shift has been done for the WAXS profiles.

Fig. 5 Peakfit treatment of meridian integrated WAXS profiles of glassy PLA (a) before stretching and (b) stretched at 50 °C up to $\varepsilon \approx 112.2\%$.

Fig. 6 Engineering stress–strain curves and evolutions with strain of mesocrystal content, X_{meso}, amorphous phase content, X_{am}, and orientation degree of amorphous chain, f_{am} computed from WAXS data of PLA upon drawing at (a) 50 °C, (b) 55 °C and (c) 60 °C.

Fig. 7 The initial strain for mesocrystal appearance, ε_{int}, varying with the logarithm of drawing temperature, $\log T_d$. The red line is the linear fitting of ε_{int} and $\log T_d$.

Fig. 8 The variations of correlation length of mesophase, ξ, mesocrystal content, X_{meso} and amorphous phase, X_{am}, of PLA stretched at (a) 50 °C, (b) 55 °C and (c) 60 °C. The correlation length of mesophase calculated from the SAXS profile of equatorial integration, ξ_e, corresponding to the value perpendicular to stretching direction, and that calculated from the SAXS data of meridional integration, ξ_m, corresponding to the one parallel to stretching direction. The variations of the ξ values in the dashed circles were influenced by the fomation and development of cavities.

Fig. 9 Schematic mechanism of the structure evolution of PLA uniaxially stretched at (a) 50 °C and (b) 60 °C. The stretching direction was horizontal.

Fig. 10 DSC traces of deformed PLA samples after stretching at 50 °C, 55 °C, and 60 °C (for the sake of comparison the DSC trace of undrawn PLA sample is also shown here. $P_{endo,}$ P_{cc} and P_{exo} are referred to the post-T_g endothermic peak, the cold crystallization exothermic peak and the small exothermic peak just prior to melting, respectively).

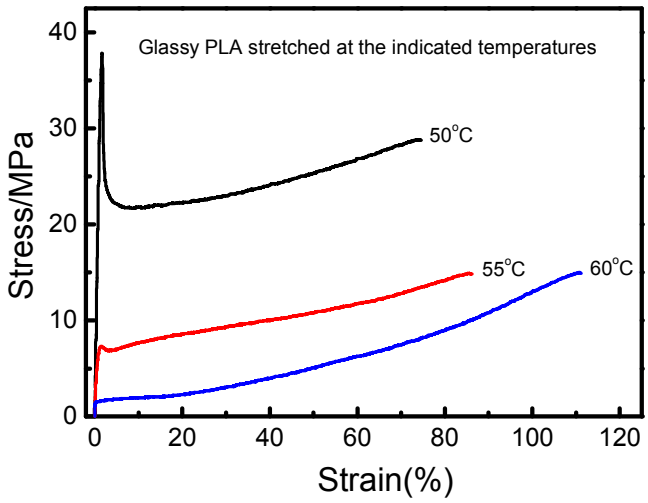

Figure 1

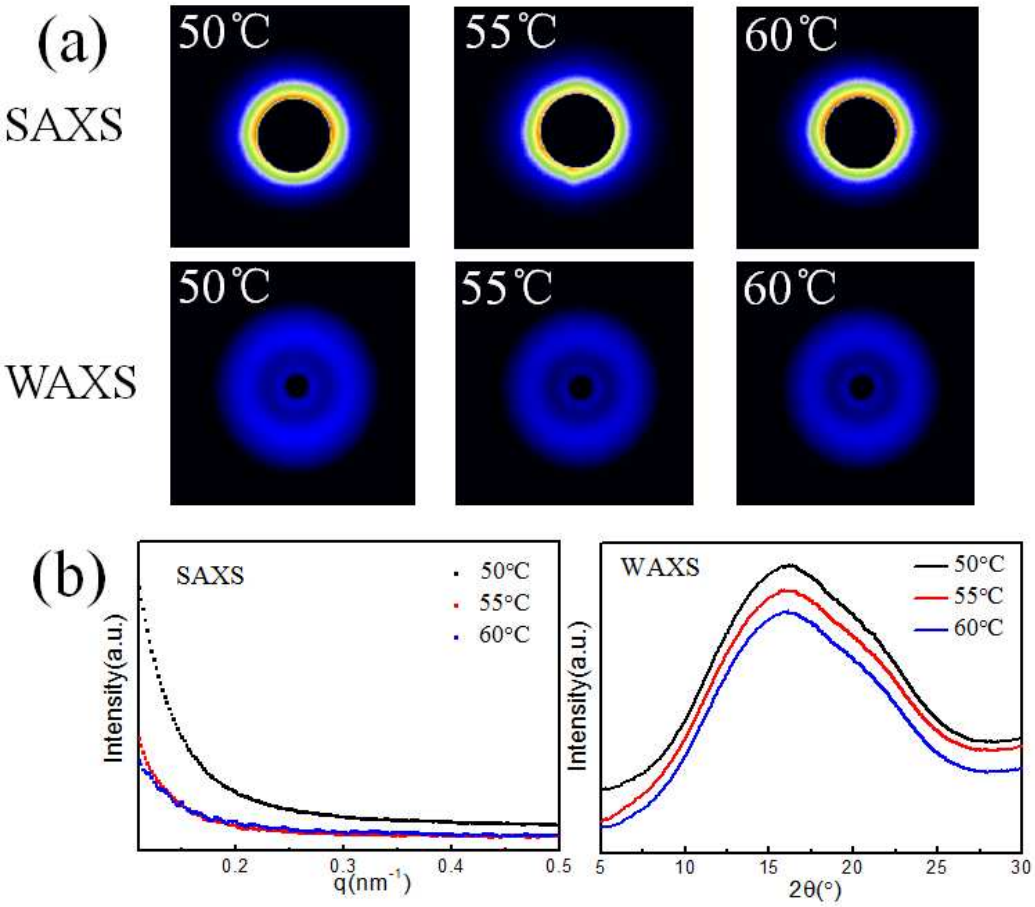

Figure 2

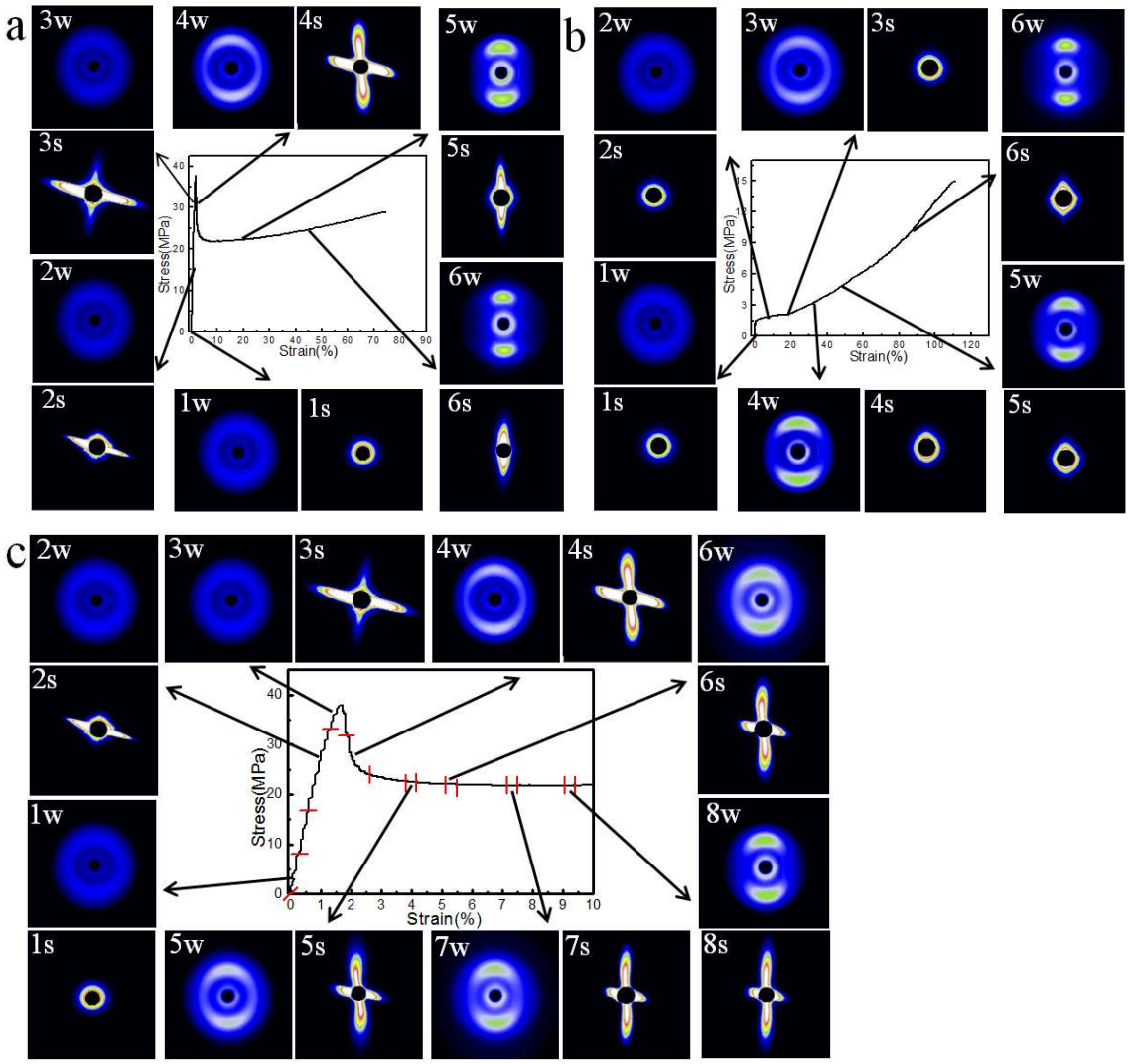

Figure 3

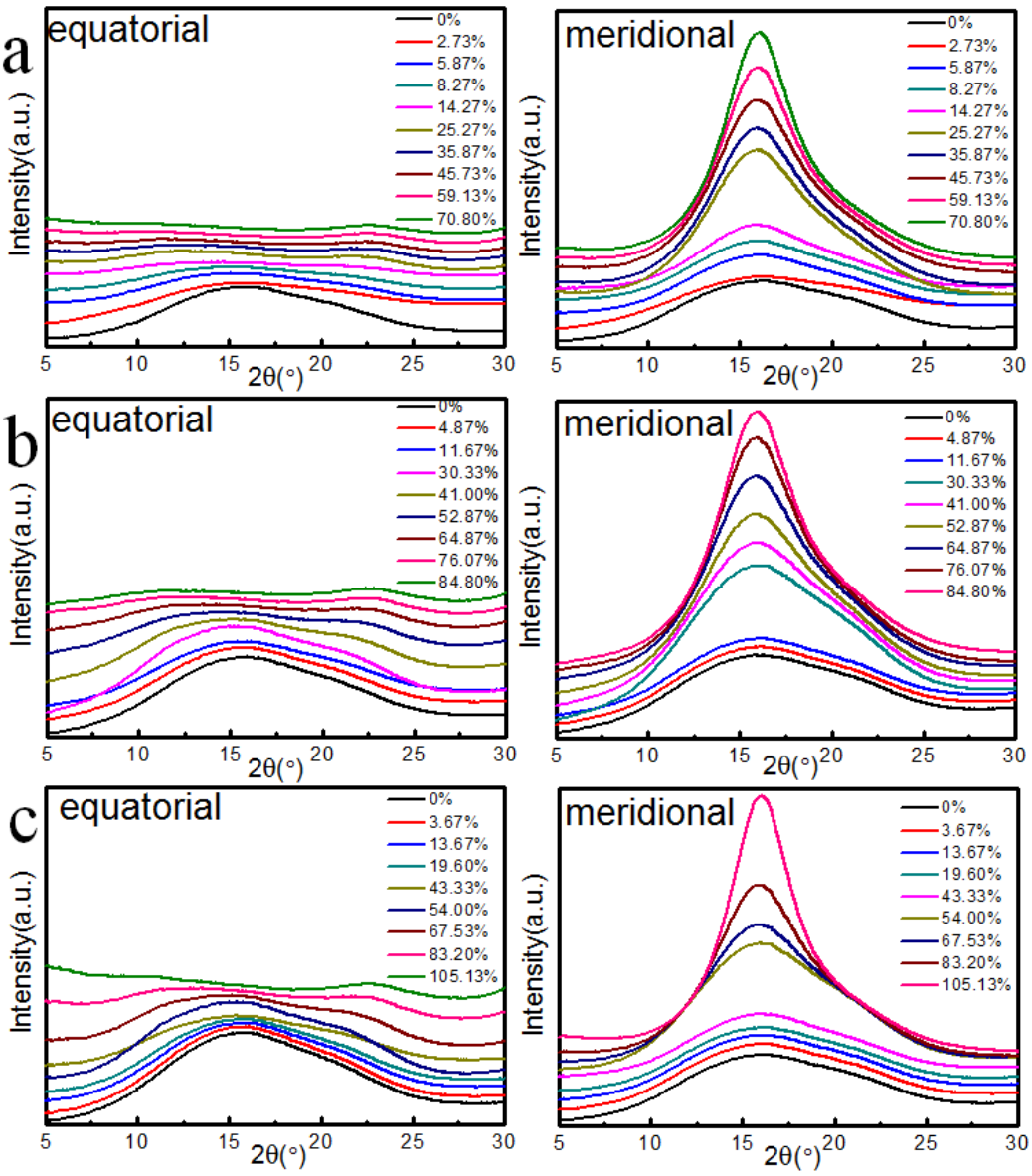

Figure 4

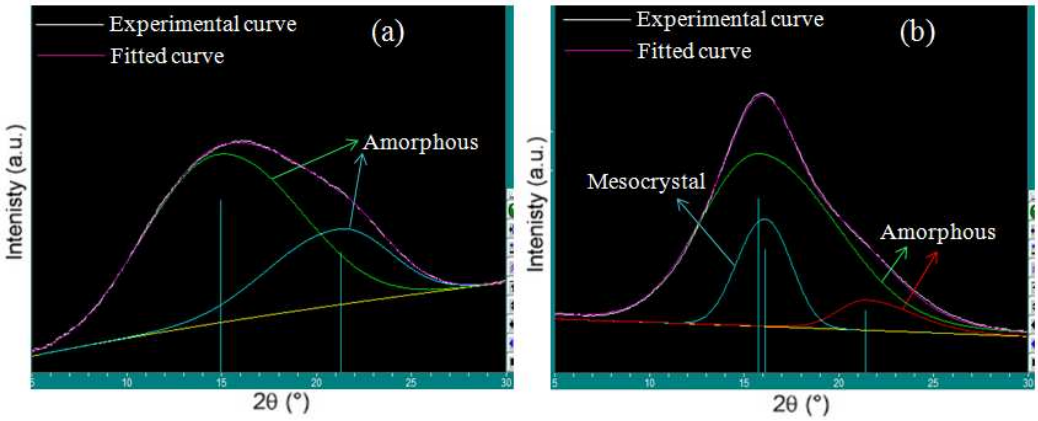

Figure 5

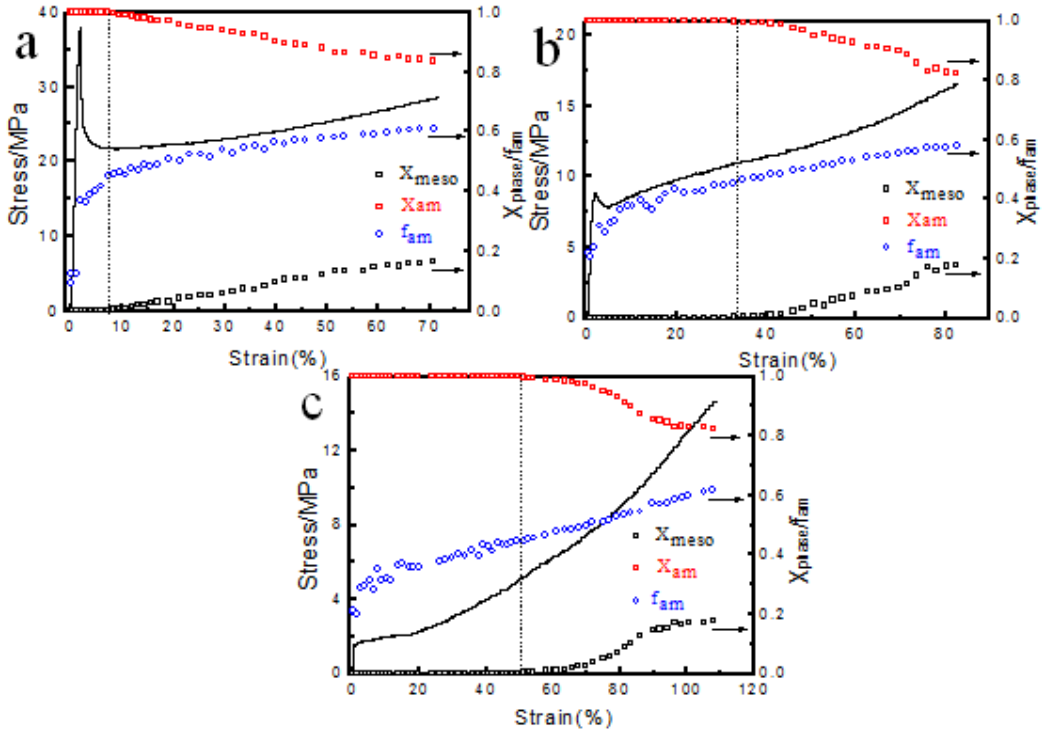

Figure 6

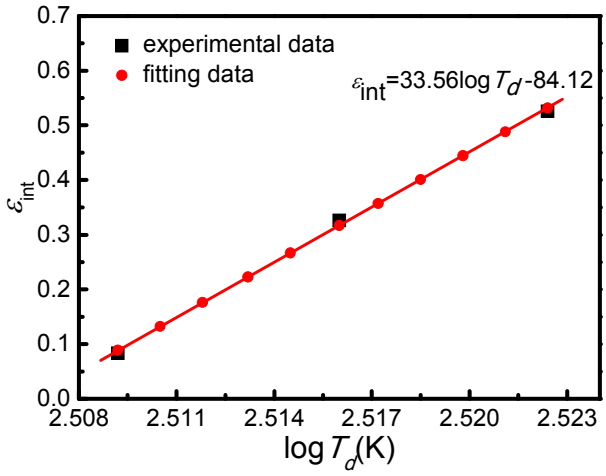

Figure 7

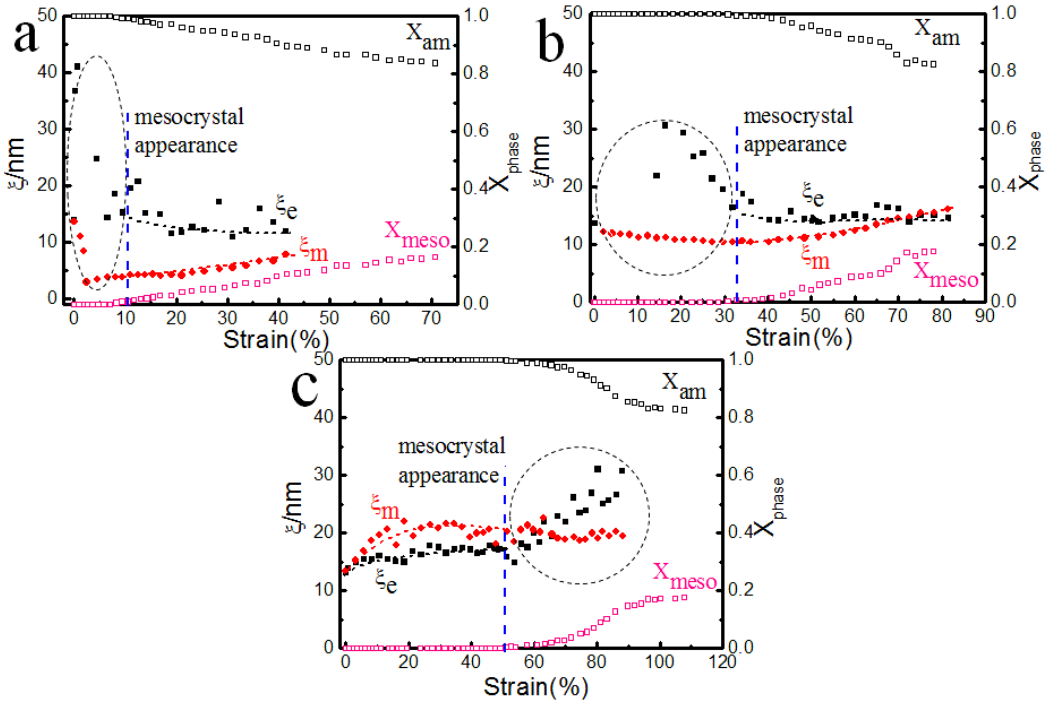

Figure 8

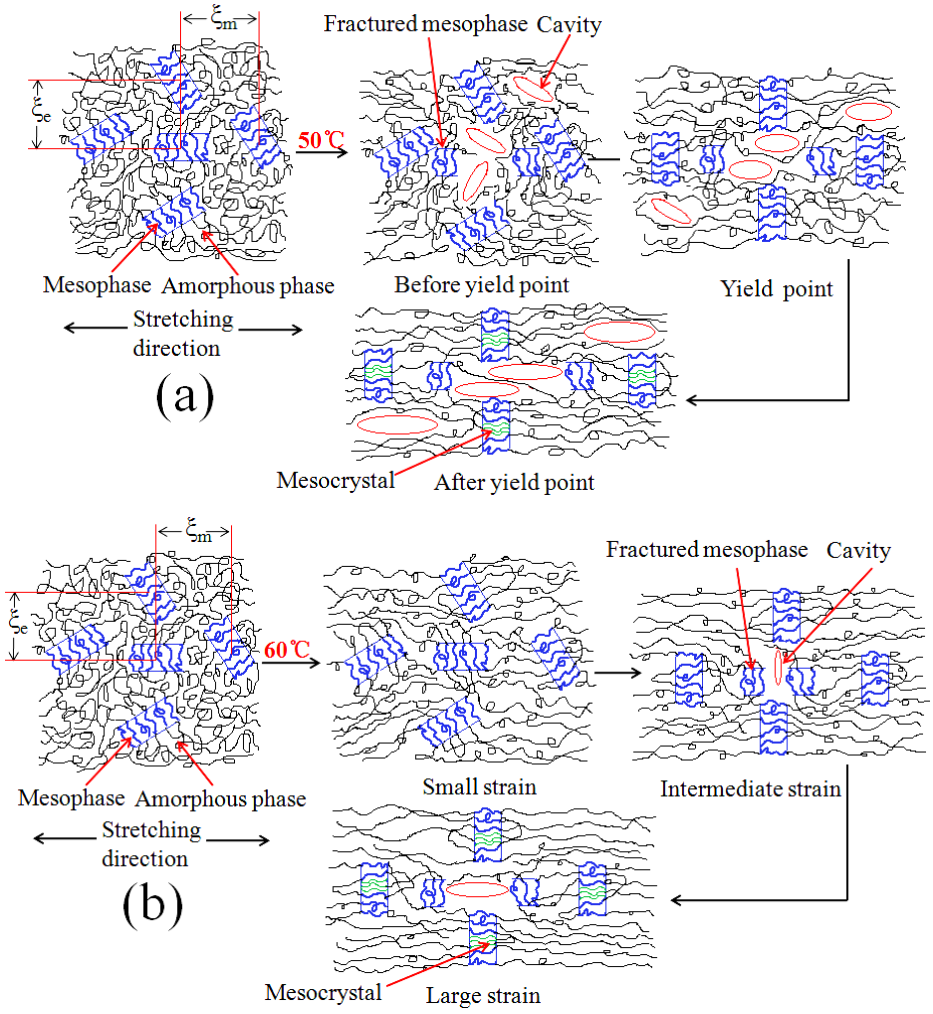

Figure 9

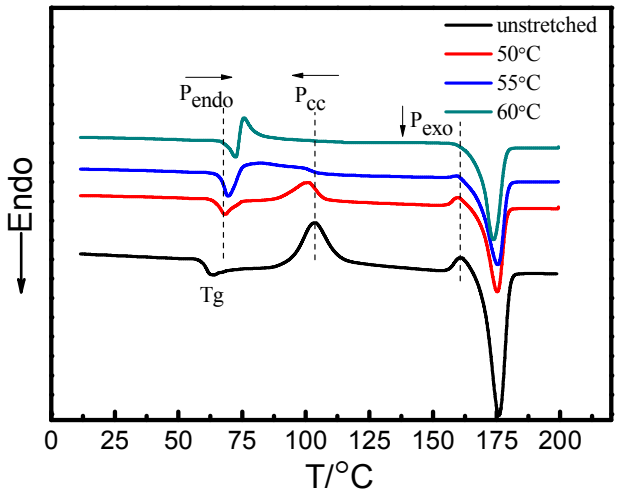

Figure 10